Unusual Proton Transfer Kinetics in Water at the Temperature of Maximum Density

Emilia V. Silletta, Mark E. Tuckerman, and Alexej Jerschow

Phys. Rev. Lett. **121**, 076001 — Published 13 August 2018

DOI: 10.1103/PhysRevLett.121.076001

Title: Unusual Proton Transfer Kinetics in Water at the Temperature of Maximum Density

Authors: Emilia V. Silletta[1], Mark E. Tuckerman[1,2,3], Alexej Jerschow[1*]

Affiliations:

[1]Department of Chemistry, New York University, New York, NY 10003, United States

[2] Courant Institute of Mathematical Science, New York University, New York, NY 10012, United States

[3] NYU-ECNU Center for Computational Chemistry at NYU Shanghai, 3663 Zhongshan Rd. North, Shanghai 200062, China

*Correspondence to: alexej.jerschow@nyu.edu

Keywords: NMR, Proton Transfer Kinetics, Water, Molecular Dynamics

ABSTRACT

Water exhibits many anomalous properties, many of which remain poorly understood. One of its intriguing behaviors is that it exhibits a temperature of maximum density (TMD) at 4ºC. We provide here new experimental evidence for hitherto unknown abrupt changes in proton transfer kinetics at the TMD. In particular, we show that the lifetime of OH^- ions has a maximum at this temperature, as opposed to the hydronium ions. Furthermore, base-catalyzed proton transfer shows a sharp local minimum at this temperature, and activation energies change abruptly as well. The measured lifetimes agree with earlier computational predictions as the temperature approaches the TMD. Similar results are also found for heavy water at its own TMD. These findings point to a high propensity of forming fourfold coordinated OH^- solvation complexes at the TMD, underlining the asymmetry between hydroxide and hydronium transport. These results could help to further elucidate the unusual properties of water and related liquids.

The study of water structure and dynamics is of particular interest due to its importance for facilitating chemical and biochemical processes that form the basis of life. It is all the more surprising that it has many anomalous and unusual properties when compared to other liquids. It stands as one of the most studied systems, and its behavior is still subject to much debate[1-2]. One of the best-known anomalous properties of water is the fact that it exhibits a density maximum at 4ºC (temperature of maximum density – TMD).

Computational work accounting for the quantum behavior of water has indicated changes in the geometry of water molecules, in particular, the O-H bond length, at the TMD[3-4]. Ramirez and Herrero[5] probed the proton kinetic energy dependence on temperature in combination with the dependence of density on temperature, as well as the influence of isotope effects. Nevertheless, accurately reproducing water's anomalous properties by remains a significant challenge[4-8]. Experimental investigations employing vibrational Raman[9] and X-ray scattering in liquid D_2O[10], suggest the presence of two competitive structures for heavy water around its TMD within the second-neighbor shell. Two major structural features were identified, with one corresponding to a more densely packed structure for second neighbors and the other indicative of an open tetrahedral network[10-12].

Charge migration in water, mediated by proton exchange between water molecules and H_3O^+ and OH^- ions has been widely investigated for its relationship to many anomalous properties. Meiboom[13] was the first to study the proton exchange kinetics in water by NMR spectroscopy as a function of pH. Subsequently, several studies have measured ^{17}O NMR linewidths as reporters of proton exchange in water[14-16]. Pfeifer calculated the exchange rates at temperatures above the TMD by ^1H spin-spin relaxation times[17], and the water proton transfer in solutions of strong electrolytes was studied via the ^1H linewidth[18]. Further work includes the

study of the pH-dependence of ^{17}O transverse relaxation rates for both H_2O and D_2O[19], the observation of non-Arrhenius behavior (mostly in the supercooled region) of ^{17}O longitudinal rates[20], and the measurement of proton exchange by means of ^{1}H field-cycling relaxometry[21]. Recently, the ^{1}H relaxation at very low Larmor frequencies was revisited using a superconducting quantum interference device (SQUID)[22]. In addition, ultrafast 2D Infrared spectroscopy has been used to investigate proton transfer in aqueous hydroxide solutions[23] and in aqueous hydrochloric acid solutions[24].

The currently accepted model is that H_3O^+ and OH^- transport is driven by hydrogen bond rearrangements that equalize coordination patterns of species on both sides of a hydrogen bond through which the fundamental proton transfer or hopping step occurs, leading to the concept of presolvation[25-26]. For H_3O^+ transport, this mechanism only requires, as a first step[26], that a first solvation-shell water lose one of its acceptor hydrogen bonds, thus changing its coordination pattern from a tetrahedral fourfold one to a threefold pattern that closely matches that of the hydronium ion. Applying the concept to hydroxide is somewhat subtler, however, as the dominant solvation pattern of hydroxide is one in which the OH^- oxygen atom accepts four hydrogen bonds in a roughly planar arrangement, termed a "hyper-coordinated" or non-Lewis like structure[27-29]. This structure, which is "inactive" with respect to proton exchange, transforms into a tetrahedral threefold pattern via loss of one of its first solvation shell members, and the structure ultimately becomes "active" when, in addition, the OH^- hydrogen donates a hydrogen bond[27-29]. This three-acceptor-one-donor (3A+1D) pattern closely matches that of its coordinating water molecules, thus promoting the subsequent proton transfer. Numerous experiments support this picture of the structural diffusion mechanism for OH^- transport in water[30-31]. Additional *ab initio* molecular dynamics studies[32] predicted an anomalous slowing

down of the hydroxide reorientation times as the TMD is approached[33], suggesting that this phenomenon is caused by an increased propensity for OH^- ions to exist in the inactive fourfold hyper-coordinated solvation state[27-28].

In this work, we report an abrupt change of the exchange rates at the TMD for both light and heavy water, measured via fine-grained temperature and pH-dependent ^{17}O NMR relaxation measurements, and specifically identify a minimum in the base-catalyzed proton exchange rates, which to the best of our knowledge has never been found before. This finding is in line with the aforementioned low-temperature *ab initio* molecular dynamics studies[32].

The proton exchange rates in water can be both acid- and base-catalyzed and the processes can be written as[13]:

$$(I)\ H_2O + H_3O^+ \xrightarrow{k_1} H_2OH^+ + H_2O$$

$$(II)\ OH_2 + OH^- \xrightarrow{k_2} OH^- + HOH$$

with the overall rate for proton transfer derived as[13]

$$k_{ex} = 1/\tau_{ex} = 2/3 k_1 10^{-pH} + k_2 K_w 10^{pH}, \qquad (1)$$

where k_1 and k_2 are the rate constants for the acid- and base-catalyzed reactions and K_w is the ion product of water[34]. Although both hydroxide and hydronium ion mobilities contribute to the proton transfer, the hydroxide ion mobility has been historically less studied. In view of the perceived asymmetry in the transfer mechanisms between hydronium and OH^-[27-29], it is particularly important to determine the individual rates of both the acid- and base-catalyzed processes separately.

While ^{17}O NMR has the disadvantage of a low natural abundance (0.0373 %), a broad resonance line, and short relaxation times due to quadrupolar relaxation, its use is advantageous because it can specifically sense the presence of the two protons via ^{17}O-^{1}H *J*-couplings. The ^{17}O

resonance frequency hops between three different positions in the triplet formed due to the ^{17}O-^{1}H *J*-couplings (~90 Hz) whenever a proton is exchanged[15]. Since the splitting is rarely detectable directly, due to fast exchange, this process is typically quantified via the average linewidth, the spin-spin relaxation time T_2, and the spin-lattice relaxation time in the rotating frame $T_{1\rho}$. The latter parameter is widely used in studies of protein dynamics,[35-36] and simple, analytical expressions for this relaxation constant exist under certain assumptions as a function of the exchange rates[37-38]. Most of these expressions are valid for a fast exchange system or in cases where there is a single dominant pool of spins exchanging with several smaller pools. Palmer et al.[35] provided these expressions for 2 or more exchange sites.

In this work, a distinct anomaly in ^{17}O T_2 and $T_{1\rho}$ is seen at the TMD. By varying the pH of water solutions, the exchange rates k_1 and k_2 can be calculated from T_2 and $T_{1\rho}$ NMR experiments. A minimum in the overall exchange rate was found at the TMD, and specifically, the base-catalyzed rate was identified as contributing most to this anomaly.

The temperature dependences of the longitudinal (T_1) and transverse (T_2) ^{17}O nuclear spin relaxation processes are shown as a function of temperature in Fig. 1 for H_2O and D_2O at pH=7. The relaxation processes are plotted as the logarithm of the respective rates, $R_1=1/T_1$, and $R_2=1/T_2$ vs. inverse temperature ($1/T$) in order to identify Arrhenius-type behavior. Linear behavior is seen for both H_2O and D_2O, except for a marked discontinuity at the TMD for R_2 for H_2O. In addition, the fitted slopes at temperatures above and below the TMD are different from each other for the R_2 curves.

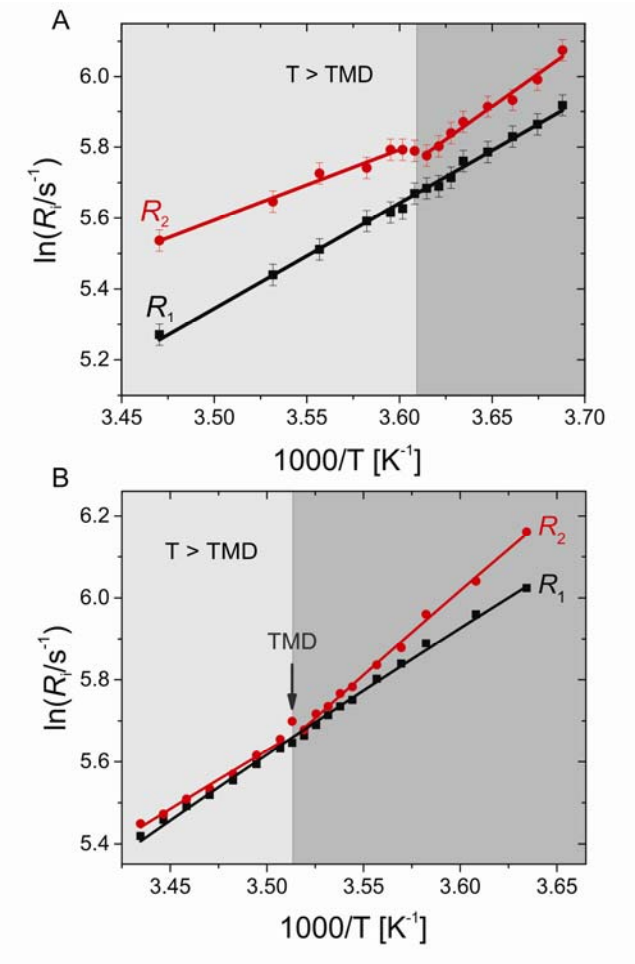

Figure 1: ^{17}O relaxation rates in water plotted as $\ln(R_i/s^{-1})$ vs inverse temperature. R_i with (i=1 or 2) refers to the longitudinal and transversal relaxation rates, respectively. The experiments were performed (A) in water at pH=7 over a temperature range from -2ºC to 15ºC and (B) in D_2O pH=7.44 where the temperature range was from 2ºC to 18ºC. The standard deviation was calculated from four independent measurements at the same temperature. The discontinuities of R_2 are supported by a statistical outlier test with 95% confidence.

Assuming a relatively constant activation energy E_a over the temperature ranges studied, we obtain E_a=24.7±0.4 kJ/mol for R_1. For R_2 above the TMD, we obtain E_a=17±1 kJ/mol, and a separate fit below the TMD gives the value of E_a=36±2 kJ/mol. The measured activation energy

for the proton R_1 process in ice is E_a=59 kJ/mol, for comparison[39]. It is reasonable that the measured values do not exceed those for ice.

When repeating the same experiment with 99.9% D_2O, the discontinuity, and change of slope were found at 11ºC, which corresponds to the TMD for heavy water. As seen in Fig. 1B, the effect is less pronounced, but nonetheless clearly visible, suggesting that influence of quantum nuclear effects in determining how pronounced the effect is. In analogy to H_2O, $\ln(R_1/s^{-1})$ exhibits linear behavior in the range studied while $\ln(R_2/s^{-1})$ shows a clear discontinuity and a significant change of slope at the TMD of D_2O; these effects lie well outside the experimental uncertainties. Table 1 shows the comparison of the extracted E_a values for both H_2O and D_2O.

	E_a of H_2O/D_2O (95/5) [kJ/mol]	E_a of D_2O [kJ/mol]
R_1	24.7 ± 0.4	25.8 ± 0.4
R_2 above TMD	17 ± 1	23.8 ± 0.8
R_2 below TMD	36 ± 2	34.7 ± 0.8

Table 1: Activation energies calculated from ^{17}O R_1 and R_2 in H_2O/D_2O (95/5) and D_2O. The activation energies derived above and below the TMD differ by more than 14 standard deviations for H_2O/D_2O (95/5), and more than 13 for D_2O (combined standard deviations are taken).

The activation energy for R_1 is higher for D_2O than for H_2O. For R_2 the trend is the same above the TMD, while it is the opposite below the TMD. This observation can be interpreted as a reflection of the presence of competing quantum effects[40], the balance of which can change as a function of temperature. In hydrogen bonds, a phenomenon known as the *Ubbelohde effect* leads to a contraction of a hydrogen bond upon replacing D^+ with H^+. This effect arises from the fact that H^+ exhibits a more pronounced quantum mechanical character in the form of spatial delocalization (mostly due to zero-point energy) in the hydrogen bond[41-43]. It is this increased

delocalization that contracts the hydrogen bond, bringing the oxygens closer together, on average, than they would be in the corresponding deuterated hydrogen bond. This contraction is tantamount to a strengthening of the hydrogen bond along the bonding direction. In directions orthogonal to the bond, however, quantum nuclear effects weaken the bond when D^+ is replaced by H^+. This occurs, for example, in the angle-bending mode due to a softening of the bend potential. At room temperature, the effects nearly cancel each other out, reducing the overall influence of nuclear quantum effects[40].

An analogous competition may occur within the hydroxide solvation complexes. At room temperature, *ab initio* molecular dynamics and *ab initio* path integral calculations suggest that proton transfer is more facile when quantum nuclear effects are accounted for. The predicted "corner cutting" results from a softening of the potential along the angular direction[29]. At temperatures above the TMD, this effect causes the activation energy associated with H^+ transfer to be lower than that of D^+. The calculations suggest that proton transfer occurs preferentially when the OH^- is in the "active" threefold-coordinated state, as discussed above. This process is shown schematically in Fig. S1 (S1A to S1B), and the donation of a hydrogen bond through the OH^- site is shown in Fig. S1C[25, 27-29]. The softening of the potential along the angular direction makes it easier for the proton to transfer when the threefold pattern is not in an ideal tetrahedral geometry. Below the TMD, however, the calculations of Ma and Tuckerman[32] suggest that fourfold hyper-coordinated complexes are more prominent, and the competition of nuclear quantum effects shifts in favor of strengthening the four hydrogen bonds around the hydroxide oxygen (Ubbelohde effect), increasing the rigidity of the hyper-coordinated complex. The shift also reduces quantum effects along the orthogonal directions. The key step in the proton transfer process, which requires that this hyper-coordinated complex transforms to the threefold complex

(Fig. S1), therefore, becomes less favorable for H^+ compared to D^+, giving rise to an increase in activation energy. This view accords with the isotope differences observed in Fig. 1.

In order to support the initial findings, rotating frame relaxation measurements ($R_{1\rho}$) were performed. These measurements, employing a spin lock pulse with adjustable radiofrequency (rf) power, allow one to scale the relative contributions of R_1, R_2 and thus tune the level of sensitivity to exchange. With these experiments, one can gauge the intermediate exchange regime more accurately[37]. This modification was necessary for the study of different pH regimes, as discussed below. Fig. 2 shows $R_{1\rho}$ curves for different rf powers ω_1 as a function of pH for different temperatures. For fast exchange (low and high pH values), $R_{1\rho}$ becomes equal to R_1, as expected, and, when ω_1 is high, $R_{1\rho}$ becomes equal to R_1 across the whole pH range. It can be seen that the $R_{1\rho}$ curves are similar to each other for $\omega_1/2\pi$=69, 139 and 278 Hz, while they start to decrease when $\omega_1/2\pi$=557 Hz. It was found that at $\omega_1/2\pi$=4500 Hz, $R_{1\rho}$ becomes insensitive to pH variations and equal to R_1. The maximum amplitude for the spin-lock field $\omega_1/2\pi$=557 Hz was chosen as a balance between sensitivity to pH and robustness against offset effects.

The higher value of $R_{1\rho}$ at 4ºC around pH=7 can be related to a minimum in the exchange process, which is also at the root of the discontinuity in the R_2 rates shown in Fig. 1. The individual acid- and base-catalyzed exchange rates can be extracted from these data by fitting a numerical model on the basis of H-hopping and associated frequency shifts due to ^{17}O-^{1}H *J*-coupling, as outlined in the Supplemental Material[44]. Fig. 2 shows the experimental results along with the fitted lines. The dip in the theoretical curves is not seen in all experimental data points in the vicinity of pH=7, which is due to an increased uncertainty in this region. The fitted exchange parameters are most sensitive to the position of the maximum of the curve, which is given by the

ratio of the two exchange parameters, and the width of the curve is linked to the geometrical average of the two rate constants. Therefore, the parameters are not very sensitive to the uncertainty in the dip region, as was also seen in earlier work[13].

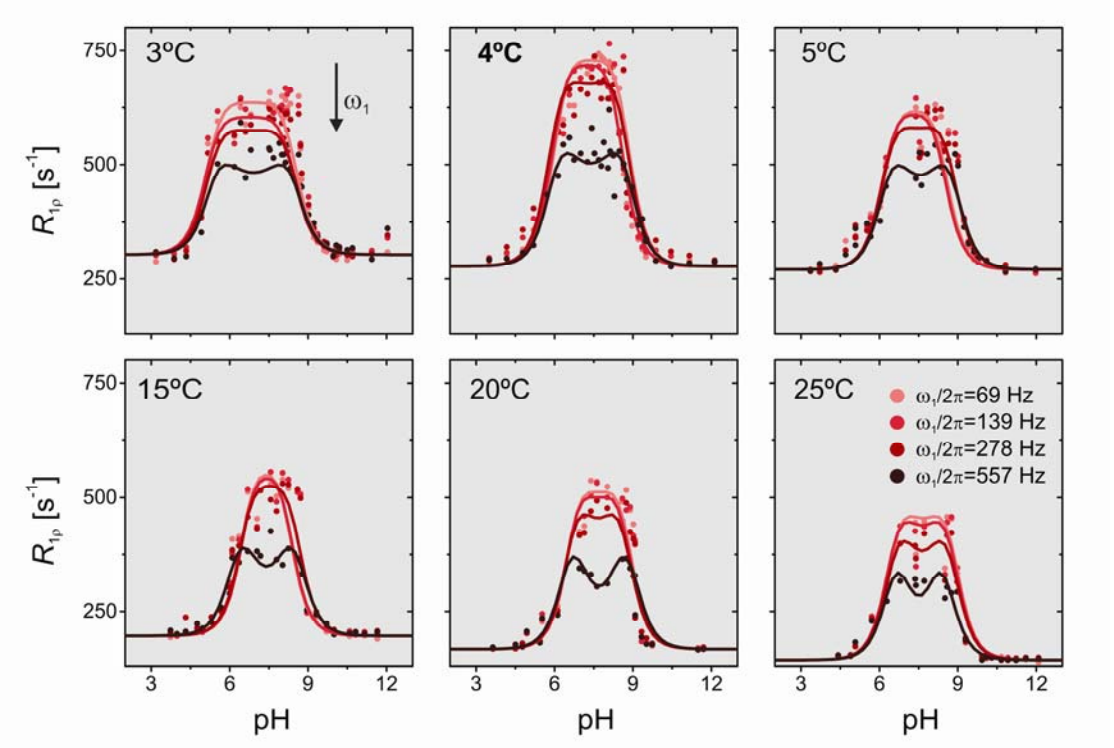

Figure 2: $R_{1\rho}$ using $\omega_1/2\pi$=69, 139, 278, and 557 Hz rf power. Dots represent the experimental data while the lines show the numerical fittings. A maximum $R_{1\rho}$ value can be observed at 4ºC around the neutral pH range. This anomaly disappears at low and high pH when the exchange is increased.

Fig. 3A shows the exchange rates k_1 and k_2 obtained from these $R_{1\rho}$ experiments. The exchange rate k_1 increases monotonically with temperature while k_2, which describes the exchange between water molecules and hydroxide, exhibits a minimum value at the TMD. In order to validate this minimum, k_2 obtained from R_2 data (Supplemental Material) is included, showing the same behavior. It is, therefore, the base-catalyzed process that is responsible for the

discontinuity in the observed values. Fig. S5 shows the total proton exchange time and exchange rate as a function of pH.

From the exchange rate k_2, the lifetime of OH^- can be calculated as $\tau=1/k_2[OH^-]$, which changes with temperature and is shown in Fig. 3B. The OH^- lifetime calculated here can be compared with Fig. 1B from reference[32] where Ma and Tuckerman calculated the reorientation time of OH^-, which is also reproduced in Fig. 3B for comparison. The results presented here are in good agreement with the theoretical calculation, where the reorientation time is at a maximum at the TMD, although in that paper, the TMD was the minimum temperature studied. A caveat is that it was not tested whether the minimum temperature of 277 K studied by Ma and Tuckerman corresponded to the actual TMD for the density functional approximation, basis set size, and pseudopotential scheme employed in their work. Importantly, Ma and Tuckerman showed that the maximum in reorientation time corresponded to a maximum in the proton exchange time (see Fig. 3 of Ref.[32]) and a minimum in the hydroxide diffusion coefficient (Fig. 4 of[32]), again in line with a high propensity of "hyper-coordinated" OH^- solvation complexes at the TMD. The "freezing in" of such high coordination complexes is consistent with the notion of the formation of a greater number of hydrogen bonds at a density maximum. Interestingly, additional computational studies have suggested that once locked in, these hyper-coordinated structures can persist into the ice phase[45-46].

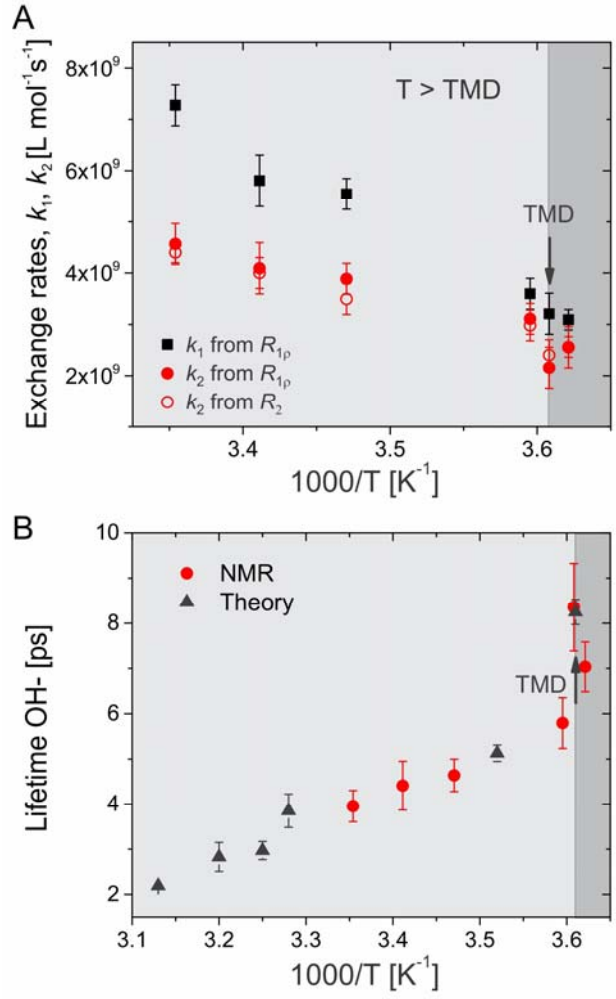

Figure 3: Exchange rates and OH^- lifetimes vs. inverse temperature. (A) Exchange rates k_1 and k_2 calculated from $R_{1\rho}$ and R_2 relaxation data. (B) OH^- lifetime calculated from k_2. The error-bars represent the standard deviation from results obtained from four separate experiments with different spin-lock fields. The error bars for k_2 calculated from R_2 data correspond to the error in the fitting. Results from theoretical calculations for the reorientation time of OH^- reproduced from Fig. 1B in Ref[32] are shown with gray triangles.

In conclusion, this work presents new experimental evidence for unusual behavior of water at the TMD, which includes a local OH^- lifetime maximum, and an abrupt change in

activation energies. Furthermore, a good agreement of these experimentally determined lifetimes is found with computationally predicted lifetimes in the approach to the TMD. These results help to elucidate the anomalous features of water and may provide further insights into proton transfer dynamics.

SUPPLEMENTAL MATERIAL

Fig. S1. Scheme for the mechanism of the transport of OH^-.

Fig. S2. Experimental R_2 values at different pH and temperature.

Fig. S3. Experimental ^{17}O $R_{1\rho}$ values at different pH and temperature

Fig. S4. Experimental linewidths at different pH and temperature.

Fig. S5. Experimentally determined proton exchange time and the exchange rate at different pH and temperature.

ACKNOWLEDGEMENT

The authors want to thank Dr. Eli Bendet-Taicher for exploring preliminary experiments. **Funding:** The work was supported by grants from the US National Science Foundation under Award Numbers CHE 1710046 (A.J.), and CHE-1534374 (M.E.T.) and partially by the MRSEC Program of the National Science Foundation under Award Number DMR-1420073. The Bruker Avance-500 NMR Spectrometer was acquired through the support of the National Science Foundation under Award Number CHE-01162222.

REFERENCES

1. Nilsson, A.; Pettersson, L. G., The structural origin of anomalous properties of liquid water. *Nat Commun* **2015,** *6*, 8998.
2. Gonzalez, M. A.; Valeriani, C.; Caupin, F.; Abascal, J. L., A comprehensive scenario of the thermodynamic anomalies of water using the TIP4P/2005 model. *J. Chem. Phys.* **2016,** *145* (5), 054505.
3. Deeney, F. A.; O'Leary, J. P., Zero point energy and the origin of the density maximum in water. *Phys. Lett.* **2008,** *372* (10), 1551-1554.
4. Paesani, F.; Iuchi, S.; Voth, G. A., Quantum effects in liquid water from an ab initio-based polarizable force field. *J. Chem. Phys.* **2007,** *127* (7), 074506.
5. Ramírez, R.; Herrero, C. P., Kinetic energy of protons in ice Ih and water: A path integral study. *Phys. Rev. B* **2011,** *84* (6).
6. Mahoney, M. W.; Jorgensen, W. L., Quantum, intramolecular flexibility, and polarizability effects on the reproduction of the density anomaly of liquid water by simple potential functions. *J. Chem. Phys.* **2001,** *115* (23), 10758-10768.
7. Noya, E. G.; Vega, C.; Sese, L. M.; Ramirez, R., Quantum effects on the maximum in density of water as described by the TIP4PQ/2005 model. *J. Chem. Phys.* **2009,** *131* (12), 124518.
8. McBride, C.; Aragones, J. L.; Noya, E. G.; Vega, C., A study of the influence of isotopic substitution on the melting point and temperature of maximum density of water by means of path integral simulations of rigid models. *Phys. Chem. Chem. Phys.* **2012,** *14*, 15199-15205.
9. D'Arrigo, G.; Maisano, G.; Mallamace, F.; Migliardo, P.; Wanderlingh, F., Raman scattering and structure of normal and supercooled water. *J. Chem. Phys.* **1981,** *75* (9), 4264-4270.
10. Bosio, L.; Chen, S. H.; Teixeira, J., Isochoric temperature differential of the x-ray structure factor and structural rearrangements in low-temperature heavy water. *Phys. Rev. A* **1983,** *27* (3), 1468-1475.
11. Cho, C. H.; Singh, S.; Wilse Robinson, G., An Explanation of the Density Maximum in Water *Phys. Rev. Lett.* **1996,** *79* (10), 1651-1654.
12. Mallamace, F.; Branca, C.; Broccio, M.; Corsaro, C.; Mou, C.-Y.; Chen, S. H., The anomalous behavior of the density of water in the range 30 K < T < 373 K. *Proc. Natl. Acad. Sci. U.S.A.* **2007,** *104* (47), 18387-18391.
13. Meiboom, S., Nuclear Magnetic Resonance Study of the Proton Transfer in Water. *J. Chem. Phys.* **1961,** *34* (2), 375-388.
14. Rabideau, S. W.; Hecht, H. G., Oxygen□17 NMR Linewidths as Influenced by Proton Exchange in Water. *J. Chem. Phys.* **1967,** *47* (2), 544-546.
15. Turner, D. L., Proton and deuteron exchange rates in water measured by oxygen-17 N.M.R. *Mol. Phys.* **1980,** *40* (4), 949-957.
16. Halle, B.; Karlström, G., Prototropic charge migration in water. Part 1.—Rate constants in light and heavy water and in salt solution from oxygen-17 spin relaxation. *J. Chem. Soc., Faraday Trans. 2* **1983,** *79* (7), 1031-1046.
17. Pfeifer, R.; Hertz, H. G., Activation Energies of the Proton-exchange Reactions in Water Measured with the 1H-NMR Spin Echo Technique. *Ber. Bunsenges. Phys. Chem.* **1990,** *94*, 1349-1351.
18. Diratsaoglu, J.; Hauber, S.; Hertz, H. G.; Müller, K. J., Water Proton Exchange Rates in Solutions of Strong Electrolytes Effected by H and OH Additions. An NMR Line Width Study. *Z. Phys. Chem.* **1990,** *168*, 13-42.

19. Richardson, S. J., Contribution of Proton Exchange to the Oxygen-17 Nuclear Magnetic Resonance Transverse Relaxation Rate in Water and Starch-Water Systems *Cereal Chem.* **1989,** *66* (3), 244-246.
20. Qvist, J.; Mattea, C.; Sunde, E. P.; Halle, B., Rotational dynamics in supercooled water from nuclear spin relaxation and molecular simulations. *J Chem Phys* **2012,** *136* (20), 204505.
21. Graf, V.; Noack, F.; Béné, G. J., Proton spin T1 relaxation dispersion in liquid H2O by slow proton-exchange. *J. Chem. Phys.* **1980,** *72*, 861-863.
22. Hartwig, S.; Voigt, J.; Scheer, H. J.; Albrecht, H. H.; Burghoff, M.; Trahms, L., Nuclear magnetic relaxation in water revisited. *J. Chem. Phys.* **2011,** *135* (5), 054201.
23. Roberts, S. T.; Petersen, P. B.; Ramasesha, K.; Tokmakoff, A.; Ufimtsev, I. S.; Martinez, T. J., Observation of a Zundel-like transition state during proton transfer in aqueous hydroxide solutions. *Proc. Natl. Acad. Sci. U.S.A.* **2009,** *106* (36), 15154-15159.
24. Thämer, M.; De Marco, L.; Ramasesha, K.; Mandal, A.; Tokmakoff, A., Ultrafast 2D IR spectroscopy of the excess proton in liquid water *Science* **2015,** *350* (6256), 78-82.
25. Marx, D.; Tuckerman, M. E.; Hutter, J.; Parrinello, M., The nature of hydrated excess proton in water. *Nature* **1999,** *397*, 601-604.
26. Berkelbach, T. C.; Lee, H. S.; Tuckerman, M. E., Concerted hydrogen-bond dynamics in the transport mechanism of the hydrated proton: a first-principles molecular dynamics study. *Phys. Rev. Lett.* **2009,** *103* (23), 238302.
27. Tuckerman, M. E.; Chandra, A.; Marx, D., Structure and Dynamics of OH- (aq). *Acc. Chem. Res.* **2006,** *39*, 151-158.
28. Marx, D.; Chandra, A.; Tuckerman, M. E., Aqueous Basic Solutions: Hydroxide Solvation, Structural Diffusion, and Comparison to the Hydrated Proton. *Chem. Rev.* **2010,** *110*, 2174-2216.
29. Tuckerman, M. E.; Marx, D.; Parrinello, M., The nature and transport mechanism of hydrated hydroxide ions in aqueous solution. *Nature* **2002,** *417*, 925-929.
30. Aziz, E. F.; Ottosson, N.; Faubel, M.; Hertel, I. V.; Winter, B., Interaction between liquid water and hydroxide revealed by core-hole de-excitation. *Nature* **2008,** *455* (7209), 89-91.
31. Hunger, J.; Liu, L.; Tielrooij, K. J.; Bonn, M.; Bakker, H., Vibrational and orientational dynamics of water in aqueous hydroxide solutions. *J. Chem. Phys.* **2011,** *135* (12), 124517.
32. Ma, Z.; Tuckerman, M. E., On the connection between proton transport, structural diffusion, and reorientation of the hydrated hydroxide ion as a function of temperature. *Chem. Phys. Lett.* **2011,** *511* (4-6), 177-182.
33. Thøgersen, J.; Jensen, S. K.; Petersen, C.; Keiding, S. R., Reorientation of hydroxide ions in water. *Chem. Phys. Lett.* **2008,** *466* (1-3), 1-5.
34. Bandura, A. V.; Lvov, S. N., The Ionization Constant of Water over Wide Ranges of Temperature and Density. *Journal of Physical and Chemical Reference Data* **2006,** *35* (1), 15-30.
35. Palmer, A. G., 3rd; Massi, F., Characterization of the Dynamics of Biomacromolecules Using Rotating-Frame Spin Relaxation NMR Spectroscopy. *Chem. Rev.* **2006,** *106*, 1700-1719.
36. Baldwin, A. J.; Kay, L. E., An R(1rho) expression for a spin in chemical exchange between two sites with unequal transverse relaxation rates. *J. Biomol. NMR* **2013,** *55* (2), 211-8.
37. Trott, O.; Palmer, A. G., 3rd, R1rho relaxation outside of the fast-exchange limit. *J. Magn. Reson.* **2002,** *154* (1), 157-60.

38. Trott, O.; Palmer, A. G., 3rd, Theoretical study of R(1rho) rotating-frame and R2 free-precession relaxation in the presence of n-site chemical exchange. *J. Magn. Reson.* **2004,** *170* (1), 104-12.
39. Barnaal, D. E.; Lowe, I. J., Proton Spin–Lattice Relaxation in Hexagonal Ice. *J. Chem. Phys.* **1968,** *48* (10), 4614-4618.
40. Habershon, S.; Markland, T. E.; Manolopoulos, D. E., Competing quantum effects in the dynamics of a flexible water model. *J. Chem. Phys.* **2009,** *131* (2), 024501.
41. Ubbelohde, A. R.; Gallagher, K. J., Acid-Base Effects in Hydrogen Bonds in Crystals. *Acta Cryst.* **1955,** *8*, 71-83.
42. Matsushita, E.; Matsubara, T., Note on Isotope Effect in Hydrogen Bonded Crystals. *Prog. Theor. Phys.* **1982,** *67*, 1-19.
43. Li, X. Z.; Walker, B.; Michaelides, A., Quantum nature of the hydrogen bond. *Proc. Natl. Acad. Sci. U.S.A.* **2011,** *108* (16), 6369-6373.
44. Hogben, H. J.; Krzystyniak, M.; Charnock, G. T.; Hore, P. J.; Kuprov, I., Spinach--a software library for simulation of spin dynamics in large spin systems. *J. Magn. Reson.* **2011,** *208* (2), 179-94.
45. Cwiklik, L.; Buch, V., Hydroxide trapped in the interior of ice: a computational study. *Phys. Chem. Chem. Phys.* **2009,** *11* (9), 1294-6.
46. Cwiklik, L.; Devlin, J. P.; Buch, V., Hydroxide impurity in ice. *J. Phys. Chem. A* **2009,** *113*, 7482-7490.
47. See Supplementary Material for activation energy calculations, which includes Ref. 48-49.
48. Hindman, J. C.; Zielen, A. J.; Svirmickas, A.; Wood, M., Relaxation Processes in Water. The Spin–Lattice Relaxation of the Deuteron in D2O and Oxygen□17 in H217O. *J. Chem. Phys.* **1971,** *54* (2), 621-634.
49. Agmon, N., Mechanism of hydroxide mobility. *Chem. Phys. Lett.* **2000,** *319*, 247-252.